ANS M&C 2021 - The International Conference on Mathematics and Computational Methods Applied to Nuclear Science and Engineering · Raleigh, North Carolina · October 3–7, 2021

DETECTION AND LOCALISATION OF MULTIPLE IN-CORE PERTURBATIONS WITH NEUTRON NOISE-BASED SELF-SUPERVISED DOMAIN ADAPTATION

A. Durrant[1], G. Leontidis[1], S. Kollias[1], L. A. Torres[2], C. Montalvo[2], A. Mylonakis[3], C. Demazière[3], P. Vinai[3]

[1]University of Lincoln
School of Computer Science, Machine Learning Group
Brayford Pool, Lincoln, United Kingdom

[2]Universidad Politécnica de Madrid
Energy and Fuels Department
Rios Rosas 21, 28003 Madrid, Spain

[3]Chalmers University of Technology
Department of Physics, Division of Subatomic, High Energy and Plasma Physics
SE-412 96 Gothenburg, Sweden

[1] aidenmdurrant@gmail.com, {gleontidis, skollias}@lincoln.ac.uk,
[2]la.torres@alumnos.upm.es, cristina.montalvo@upm.es
[3]{antonios.mylonakis, demaz, vinai}@chalmers.se

ABSTRACT

The use of non-intrusive techniques for monitoring nuclear reactors is becoming more vital as western fleets age. As a consequence, the necessity to detect more frequently occurring operational anomalies is of upmost interest. Here, noise diagnostics — the analysis of small stationary deviations of local neutron flux around its time-averaged value — is employed aiming to unfold from detector readings the nature and location of driving perturbations. Given that in-core instrumentation of western-type light-water reactors are scarce in number of detectors, rendering formal inversion of the reactor transfer function impossible, we propose to utilise advancements in Machine Learning and Deep Learning for the task of unfolding. This work presents an approach to such a task doing so in the presence of multiple and simultaneously occurring perturbations or anomalies. A voxel-wise semantic segmentation network is proposed to determine the nature and source location of multiple and simultaneously occurring perturbations in the frequency domain. A diffusion-based core simulation tool has been employed to provide simulated training data for two reactors. Additionally, we work towards the application of the aforementioned approach to real measurements, introducing a self-supervised domain adaptation procedure to align the representation distributions of simulated and real plant measurements.

KEYWORDS: neutron noise, machine learning, core diagnostics, core monitoring

1. INTRODUCTION

With an ageing western fleet of light-water reactors (LWRs) consequently resulting in more frequent operational anomalies, there is a necessity to ensure that accurate core monitoring is in place to appropriately detect and identify anomalies. Specifically, we investigate the use of the powerful and non-intrusive technique of noise diagnostics, the analysis of small stationary deviations of the local neutron flux from its time-averaged value. However, this relies on the non-trivial task of deriving the nature and location of the driving perturbation/anomaly — referred to as unfolding — from a scarce number of in-core instrumentation. Given the difficulty of inverting the reactor transfer function under limited instrumentation with conventional techniques, we utilise the power of Machine Learning (ML) to approximate this function from data itself.

The adoption of ML in the field of core diagnostics has, in recent times, become more prevalent with the acceptance and applicability of ML and Deep Learning (DL) advancements. Recent work has demonstrated the potential of anomaly detection via ML, where time series analysis [1] methodologies have shown great promise identifying and classifying anomalies with low error. For neutron noise based non-parametric unfolding techniques and perturbation characterisation, earlier efforts of the present authors [2–4] demonstrate the capability and effectiveness of such DL approaches considering single perturbation scenarios. This work presents an extension to the former, employing a voxel-wise, fully-convolutional, semantic segmentation network for the classification and localisation of multiple, simultaneously occurring anomalies.

However, the ability to unfold the reactor transfer function via ML, gradient based algorithms, relies on the acquisition of large quantities of training data covering all possible anomalous scenarios. To train the proposed supervised algorithms, datasets are needed for which a known perturbation type and source is assumed, and subsequently its resulting induced neutron noise estimated for a corresponding number of detectors. To obtain such a dataset encapsulating various types of known perturbations originating at all possible locations, a frequency domain modelling tool CORE SIM+ [5] is employed. These simulations provide an extensive training set comprised of single perturbation noise sources which we additively combine.

In this work we consider the vital challenge of identifying multiple, and simultaneously occurring in-core perturbations, characterising each by type and locating the position in which they originate within the core volume. The rationale is that in reality, perturbations within the core rarely occur in isolation. As such, in order to appropriately classify operation anomalies from real plant readings, we propose a voxel-wise, fully-convolutional, semantic segmentation network capable of making predictions at all positions within the core simultaneously. Furthermore, this is achieved through a limited number of neutron detectors in 2 reactors, namely a Swiss and German pre-KONVOI reactor, each taken as an application example. It is worth noting that this implementation does not consider the case that noise sources from separate perturbations originating from the same position co-exist. Moving towards the applicability of our approach to real measurements, we propose the use of Domain Adaption (DA) to minimise the inherent shift in data distributions between simulated and real measurements. This encourages our network to align data representations allowing full utilisation of vast quantities of simulated data when predicting with plant measurements.

2. MODELLING AND PROCESSING OF NEUTRON NOISE SIMULATIONS

The CORE SIM+ [5] modelling software used to generate training sets for the ML methods, estimates the effect of stationary perturbations in macroscopic cross-sections onto the neutron flux using the two-group diffusion approximation, in linear theory and assuming one group of delayed neutrons. The spatial discretization of the balance equations is based on finite differences in Cartesian geometry. Depending on the problem of interest, different numerical methods and non-uniform computational meshes can be selected for effective numerical performance and accuracy. The modelling of the corresponding noise source for the below scenarios is described in detail in [6] and [3]. From the spatial dependence of the induced neutron noise estimated by CORE SIM+, the Cross-Power Spectral Densities (CPSD) of the relative neutron noise (compared to the static neutron flux) between pairs of neutron detectors were calculated. Calculating the CPSD ensures consistency between the simulations and the type of quantities determined from the analysis of measured plant data. In this work, a Swiss 3-loop and a German 4-loop pre-KONVOI reactor are modelled using proprietary data, in order to appropriately reproduce the nuances of real measurements. Several scenarios of anomalies are considered [*], with the resulting neutron noise estimated:

- Generic "absorber of variable strength", where a spatial Dirac-like perturbation is assumed. All possible locations of the perturbation are considered.
- Axially travelling perturbations at the velocity of the coolant flow, where a perturbation is created at some spatial location in the core and travels upwards with the flow through the core. All possible locations of the perturbation are considered.
- Fuel assembly vibrations, for which the lateral movement of fuel assemblies is modelled according to the following modes of vibrations: the cantilevered beam mode, the simply supported on both sides mode (with its two first harmonics), and the cantilevered beam and simply supported mode (with its two first harmonics). All possible locations of vibrating fuel assemblies are modelled.
- Control rod vibrations, where a partially inserted control rod is assumed to laterally vibrate in the core. All possible locations of the vibrating control rod are considered.
- Core barrel vibrations, where the core barrel is assumed to vibrate in the beam or pendular mode.

Our goal is to train and evaluate ML algorithms on samples comprising of the noise response from multiple perturbations occurring simultaneously. To achieve this, we additively combine the single perturbation volumetric samples produced via CORE SIM +. Additive combination however, assumes that all vibrations are in phase and that their relative weight are kept at their respective nominal value. More appropriate and computationally efficient combination procedures are reserved for future work. For our experimentation we produce 3 combined data sets, each differing in maximum number of combinations. The number of combined single perturbations per sample is selected at random within the range $[1, x]$, where $x = \{15, 30, 45\}$, whilst ensuring that samples combinations are of the same frequency and do not originate from the same location.

In order to represent our simulated data as close to real plant measurements, and to provide our ML algorithms with rich input information, pre-processing of the volumes of induced neutron readings was undertaken. The approach follows that of [4,3], in which detailed pre-processing procedures

[*]Scenarios abbreviations: AVS = Absorber of Variable Strength, CANT = Fuel Assembly Vibration (FAV) Cantilevered, SF = FAV Supported First, SS = FAV Supported Second, CSF = FAV Cantilevered Supported First, CSS = FAV Cantilevered Supported Second, CR = Control Rod Vibration, TP = Travelling Perturbation, BV = Core Barrel Vibration, BG = Background / No Class

are given. To summarise, the Auto-Power Spectral Densities (APSDs) and CPSDs of simulated neutron detector readings are computed per single perturbation scenario, the additive combination is performed on the APSD/CPSD of the detector readings. As stated, this method introduces complications due to cross-correlation of noise. However, the combination of noise before this stage is not in the scope of this work. Given these readings are complex values, we decompose each into their amplitude and phase to allow for compatibility with DL frameworks. The input into the network are volumes of dimensions $17 \times 17 \times 17$ and $16 \times 16 \times 21$ for the German and Swiss reactors, respectively. The input volumes are half the dimension of that modelled CORESIM+, we undertake this simple reduction to reduce computation without compromising localisation. The reactors are provided with 44 and 56 detectors respectively. APSD and coherence's of these detectors are embedded into each volume at their corresponding locations, all other voxels are zero. We concatenate all volumes (amplitude and phase of APSDs and coherence's) channel-wise. Note that we do not use the coherence's between all detectors as this results in large numbers of channels, and thus computational inefficiency. We empirically found that 8 selected detectors are adequate, calculating the coherence between each detector and the 8 selected detectors, resulting in 16 channels (8 detectors each with an amplitude and phase component concatenated).

3. VOXEL-WISE SEMANTIC SEGMENTATION FOR CLASSIFICATION AND LOCALISATION OF MULTIPLE, SIMULTANEOUSLY OCCURRING ANOMALIES

To unfold and consequently characterise and localise multiple perturbations, we use a 3D Fully-Convolutional Neural Network (FCNN) to provide spatial feature extraction of the detector readings embedded in the input volume. Specifically, we task our neural network to minimise the cross entropy between a voxel-wise prediction and ground truth (the true source location of the simulated perturbations) semantic labels. This task known in computer vision as semantic segmentation, involves "linking" each voxel in the input volume to a semantic label in an output prediction volume. In our case each semantic label represents the perturbation scenario, with its location in the volume (i, j, k) representing where this perturbation originated, thus localising and classifying.

3.1. Model Description

Our proposed network — depicted in Figure 1 — follows an encoder-decoder structure, the encoder extracts and constructs high-dimensional spatial feature representations of the frequency domain input volume, whilst the decoder utilises these features to construct a prediction mask with the same dimensions as the input. Both the encoder and decoder are constructed of 3D CNN layers providing translational invariance, ideal for learning the spatial information that can vary in position throughout the volume. The model proposed is inspired from [7], taking the notable design feature of the spatial pyramid pooling block (four bottom blocks of the network). This block learns rich semantic features at various scales, using four CNN layers with differing kernel size, stride, and dilation to capture varying information at different granularities. Additionally, to capture greater spatial information given the limited number of detectors, dilated convolutions [8] are employed to increase the receptive field of the convolution operator whilst maintaining computational efficiency. Furthermore, CoordConv [9] is also implemented to help preserve spatial information of the features. This informs the convolution kernels where they are in relation to the input volume, introducing layer-wise cartesian coordinates of voxel positions, improving segmentation accuracy by $\approx 2\%$ per perturbation class.

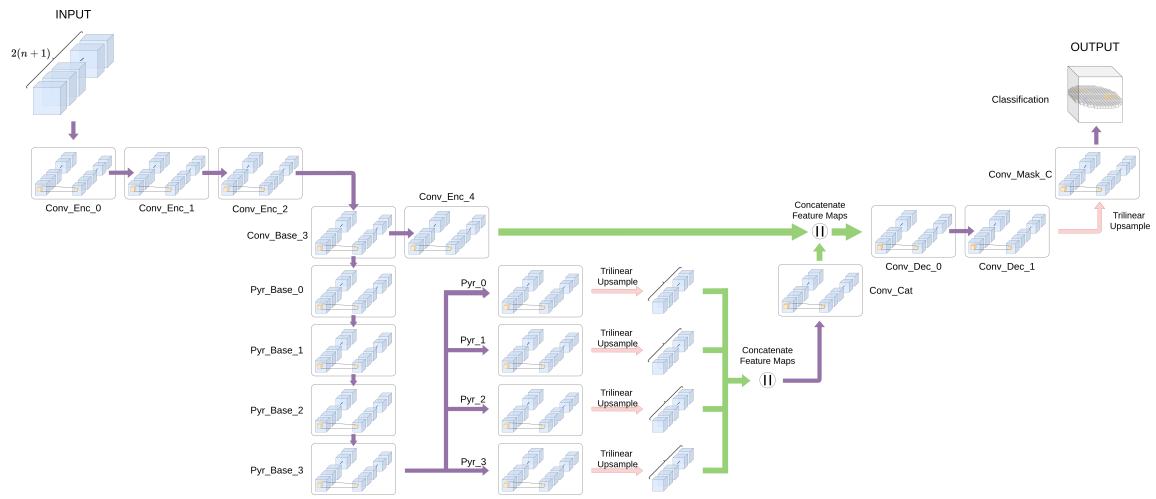

Figure 1: The proposed 3D Fully-convolutional, voxel-wise semantic segmentation network. Arrows represent the direction of network activation's, purple arrows are the flow of activation's with no operation, red show trilinear up-sampling, and green are the concatenation of activation's channel-wise.

As previously stated, the network is trained to minimise a variation of the cross entropy loss, focal loss [10]. The focal loss (Equation 1) introduces a tuneable focusing parameter, γ, to the cross entropy loss to adjust the rate at which easy examples are down-weighted and hard examples are given more significance. Here, P represents the number of perturbation classification scenarios. The rationale behind this implementation is that given the constraints of inherent reactor design, there are of course far fewer cases of a control rod vibration in comparison to examples representing a generic absorber of variable strength. As such there is an imbalance between class occurrence, where without weighting schemes the under-represented classes will not receive as much weighting in the training procedure. To further assist with class imbalance, a logarithmic class weighting scheme from [7] has been employed. The loss function is weighted per class, α_p, depending on the true class using logarithmic weighting.

$$\mathcal{L}_{FL}(y,\hat{y}) = -\frac{1}{P}\sum_{p=1}^{P}\left[y_p\alpha_p(1-\hat{y}_p)^{\gamma}\log(\hat{y}_p) + (1-y_p)(1-\alpha_p)\hat{y}_p^{\gamma}\log(1-\hat{y}_p)\right] \tag{1}$$

3.2. Simulated Measurement Experimental Results

To demonstrate the performance of our approach, experimentation has been undertaken on combinations of simulated scenarios for both a Swiss pre-KONVOI and a German pre-KONVOI reactor which were described in section 2. Our experimentation aims to explore how our approach classifies and localises each of the induced perturbations, given a range of simultaneously occurring perturbations per sample. The networks remain identical throughout, only changing the input dimensions to accommodate different reactor dimensions. The training procedure utilised the Stochastic Gradient Descent (SGD) optimisation procedure for back propagation, with a base learning rate of 0.01, decaying by a factor of 0.1 when the validation error plateaus for 20 epochs

within a threshold of 0.025. Additionally, training lasted 150 epochs with a batch size of 128, and employed ℓ-1 weight regularisation of 0.001. Furthermore, a modulating factor of $\gamma = 2$ for the focal loss was used. The percentage accuracy of our predictions are shown in Table 1, where the accuracy is defined as the percentage of correctly classified voxels per perturbation classification throughout the volume, averaged across the test set. In addition, normalised confusion matrices showing the performance per classification are depicted in Figure 2.

Per Class Voxel Accuracies on Simulated Test Sets											
Reactor	**Max No. Comb**	**Accuracy (%)**									
		BG	AVS	CANT	SF	SS	CSF	CSS	CR	TP	BV
German	**15**	**99.08**	**90.47**	**92.98**	**86.49**	**93.02**	**97.62**	**97.22**	**83.06**	**94.74**	**100.00**
German	30	99.64	85.97	81.48	90.48	97.37	90.24	95.12	90.21	93.25	100.00
German	45	99.35	82.28	88.00	87.50	89.23	90.00	92.42	88.99	93.20	100.00
Swiss	**15**	**99.43**	**87.64**	**89.47**	**82.14**	**82.93**	**89.66**	**86.11**	**93.05**	**91.16**	**100.00**
Swiss	30	99.68	84.45	83.72	92.86	86.54	86.49	81.63	87.85	90.48	100.00
Swiss	45	99.11	80.95	79.41	82.50	90.79	85.71	90.14	89.86	91.81	100.00

Table 1: Per classification voxel accuracies averaged across the unseen test set for varying numbers of combined perturbations for both simulated pre-KONVOI reactors.

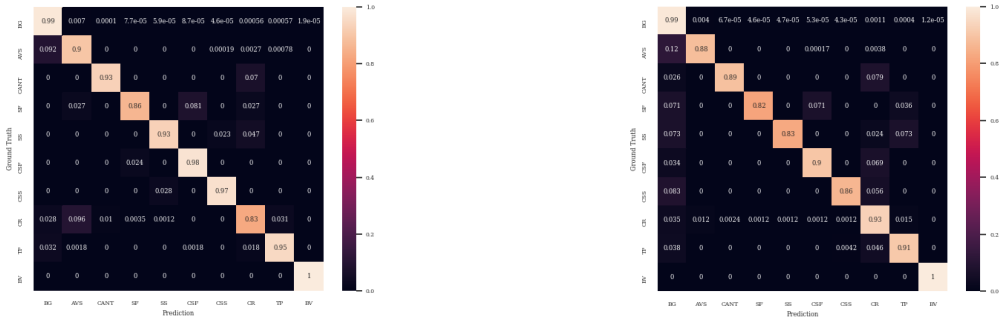

Figure 2: Normalised confusion matrix of per voxel classification on the simulated test set, max combination = 15. These show the number of voxel predictions per classification against the ground truth. (Left) German pre-KONVOI, (Right) Swiss pre-KONVOI.

Table 1 shows the results of voxel-wise classification of simultaneously occurring perturbations, and subsequently their origin locations. Low error is reported across all scenario types and combinations for each reactor type, this is further depicted by the normalised confusion matrices shown in Figure 2. It is often noticed the loss in performance is attributed to false positive predictions, i.e. detecting a perturbation that is not present. Simply put, our network tends to make additional predictions around the ground truth value, forming a cluster of predictions, this is depicted in Figure 3. Although affecting performance of our network, this result does in fact, inspire greater confidence in contrast to the contrary of false negative predictions (missed predictions). Furthermore, it is worth noting that the increase in combined perturbations per sample does result in a drop in classification performance of the more localised perturbations such as the generic absorber of variable strength, -7%. We conjecture that due to the more uniform structure of fuel assembly vibrations, control rod, and core barrel vibration,s there are fewer variations at which these perturbations can originate, thus resulting in a lower complexity in comparison to generic absorber of

variable strength.

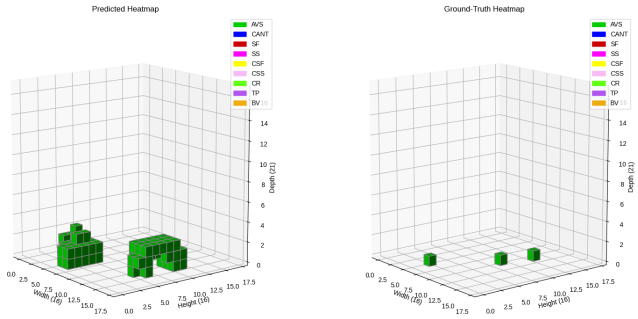

Figure 3: Network prediction (Left) and ground truth (Right) classification masks for a combination of simulated scenarios. The pressure vessel is not depicted for visual clarity.

4. SELF-SUPERVISED DOMAIN ADAPTATION FOR SYNTHETIC-TO-REAL REPRESENTATION ALIGNMENT

Given the low error of our model in synthetic case, the desirable next step is the application to real plant measurements. However this is non-trivial, since ground truth values for the real plant measurements are unknown and few in number of samples, thus we must employ the simulated data solely to learn the characteristics of the perturbations. Additionally, the simulations and real plant measurements — although fundamentally and theoretically represent the same response to anomalous phenomena — present some naturally occurring differences in data distributions. Consequently, it is necessary that mitigations are introduced to enable the large quantities of simulated data to be fully exploited for use with real plant measurements. Without such alleviation, the difference in distribution will yield a difference in feature distribution captured by the model resulting in poor predictions when inference is performed using a model trained only with simulated data.

4.1. Model Description

To align the data domains (simulated or real), we propose to utilise a domain adaptation procedure encapsulating our 3D FCNN model, to more closely align representations of the input volumes produced by our network from each data domain. Specifically, we employ the Self-Supervised Domain Adaptation (SSDA) procedure proposed in [11]. Given we do not have any labelled (ground truth) information for real plant measurements, auxiliary tasks — constructed from solely the input volumes — are employed to provide feature understanding of structurally relevant information that does not require human annotated labels. These tasks encourage alignment between the distribution of features captured by the FCNN of both the simulated (source) and real measurements (target) domains, by making the feature extractor predict identical augmentations to each input volume, hence enforcing invariance to the nuances displayed between the data distributions.

The proposed method aims to simultaneously train our previously described network to minimise the error of the main task of semantic segmentation for source domain data (simulated), whilst also minimising the loss of a variety of auxiliary tasks for both source and target (real) domains. Auxiliary tasks are simply Softmax classification tasks aiming to predict augmentations applied

identically to each of the source and target domain input samples. The tasks include: rotation prediction $[0°, 90°, 180°, 270°]$; vertical flip prediction $[0, 1]$; and prediction of a missing detector. The output for each task, including the segmentation task, is provided by individual classification layers where input is provided by the feature extractor, this is visually depicted in Figure 4. The resulting loss is the mean of the categorical cross entropy loss for each auxiliary tasks per domain, and the segmentation loss for the source domain (Equation 1). At inference time, the target test samples are input to the feature extractor, a resulting prediction mask is produced via the segmentation task head, whilst disregarding all auxiliary heads. Real plant predictions are shown in Figure 6.

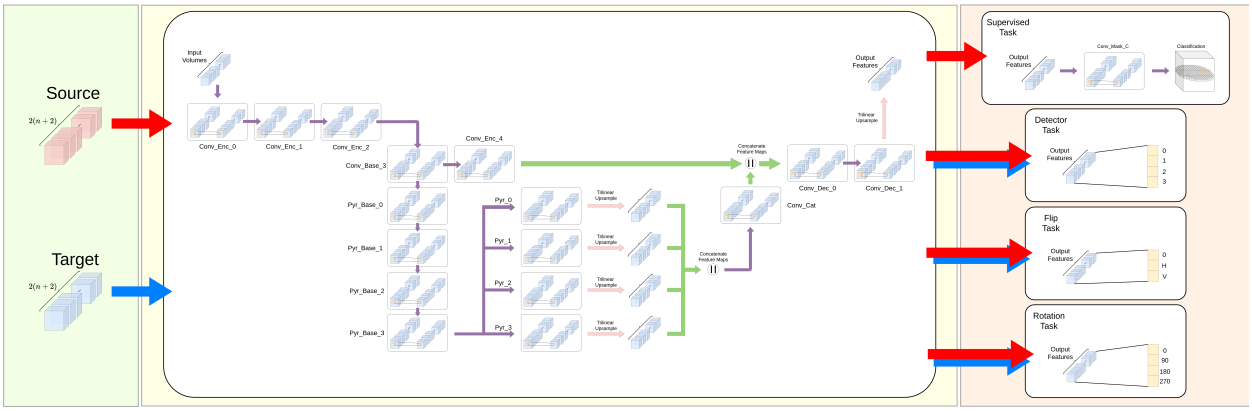

Figure 4: SSDA methodology depicting the input volumes (Left), FCNN network (Middle), and the three auxiliary tasks and supervised (segmentation) task (Right). The flow of source and target data is given by the red and blue arrows respectively.

4.2. Real Plant Measurement Experimental Results

To make predictions via our self-supervised domain adaptation procedure, the model had been trained in a similar manner as described in Section 3.2, although, for a fewer 100 epochs, weight decays of 10^{-5}, and with a smaller base learning rate of 0.001. To further leverage the simulated training, our FCNN feature extractor weights are initialised with those corresponding to the trained model from the simulated experiments, and all parameters fine-tuned throughout the domain adaptation procedure. The real plant measurements have been processed by using classical signal processing techniques for neutron noise diagnostics, observing the response of the neutron detector sensors in the frequency domain through the Fourier transform of the auto-correlation function, APSD. Analogously, for two variables, the CPSD has been calculated through the Fourier transform of the cross correlation between signals of two detectors. Moreover, to provide further information via signal processing, the coherence is calculated between detectors, by the same procedure described in Section 2.

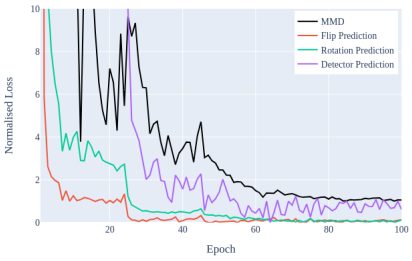

Figure 5: Normalised auxiliary task errors and MMD error between the source and target distributions. Improved alignment is shown as errors decrease until convergence.

First, Figure 5 depicts the smooth convergence of our auxiliary task losses, along with the minimisation and convergence of a non-optimised distance metric between source and target representations. This metric, measures the centroid distance (linear maximum mean discrepancy (MMD)) between the feature distributions of the two domains in the learned representation space produced by the FCNN feature extractor. This empirically shows maximisation of alignment in representational space between simulated and real domains, consequently improving invariance between source and target in our feature extractor. Additionally, Figure 6 shows the predictions made by our network for real measurements of an operational German pre-KONVOI reactor. These results, although yet to be fully validated given the inability to acquire ground truth values, show the potential of our method to make on-line predictions of core anomalies in operational reactors. To further support our claims, work by [12] undertook an alternative approach on the same real reactor measurements with similar phenomena reported at near identical locations within the core volume. For example, strong axially travelling perturbations are reported at $(12, 16)$ in [12], with our prediction (Figure 6) also reporting the same phenomena at $(14, 14)$ in addition to an axial column of generic absorber of variable strength, adding further weight to the validity of our prediction.

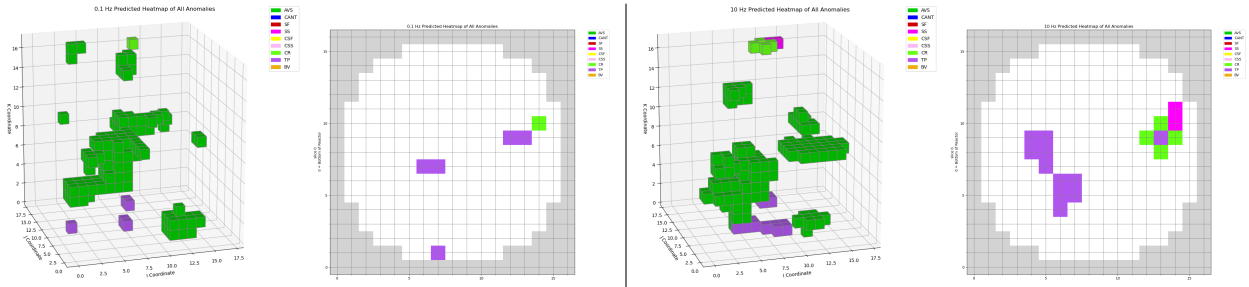

(a) 0.1 Hz **(b) 10 Hz**

Figure 6: Predictions of German pre-KONVOI reactor measurements under our self-supervised domain adaptation procedure. Left: 3D prediction visualisation of the whole core volume, we omit the reactor pressure vessel for visual clarity. Right: Axial (top down) view of the predictions excluding AVS. Outside of the pressure vessel is depicted in grey.

5. CONCLUSION

We demonstrate a method to provide novel insights into operational reactor core anomalies, achieving low error for two reactors in the simulated case with our proposed semantic segmentation network classifying and subsequently localising the origin of up to 45 simultaneously occurring perturbation scenarios. In addition, we extend this methodology to show the applicability of such a method to real plant measurements, making the non-trivial step towards leveraging large quantities of synthetic data to unfold and therefore classify and localise the origin of anomalies in real, operational reactors. Although the predictions are not yet validated, we provide empirical evidence of the minimisation of simulated and real data distributions in feature space showing the ability to adapt to the real domain from large quantities of synthetic data. Work is ongoing to further validate our predictions and extend our approach to retrieve more perturbation characteristics to provide greater details of anomalous signals. The exploration of ML and DL in nuclear safety is still relatively unexplored, with our work proposing one avenue to provide highly accurate assistance through ML predictions to analyse and form intuitions of behaviours during reactor operation.

ACKNOWLEDGEMENTS

The research conducted was made possible through funding from the Euratom research and training programme 2014-2018 under grant agreement No 754316 (CORTEX project).

REFERENCES

[1] M. Kim, E. Ou, P.-L. Loh, T. Allen, R. Agasie, and K. Liu. "RNN-Based online anomaly detection in nuclear reactors for highly imbalanced datasets with uncertainty." *Nuclear Engineering and Design*, **volume 364**, p. 110699 (2020).

[2] F. D. S. Ribeiro, F. Calivá, D. Chionis, A. Dokhane, A. Mylonakis, C. Demaziere, G. Leontidis, and S. Kollias. "Towards a deep unified framework for nuclear reactor perturbation analysis." In *2018 IEEE symposium series on computational intelligence (SSCI)*, pp. 120–127. IEEE (2018).

[3] C. Demazière, A. Mylonakis, P. Vinai, A. Durrant, F. De Sousa Ribeiro, J. Wingate, G. Leontidis, S. Kollias, et al. "Neutron Noise-based Anomaly Classification and Localization using Machine Learning." PHYSOR (2020).

[4] A. Durrant, G. Leontidis, and S. Kollias. "3D convolutional and recurrent neural networks for reactor perturbation unfolding and anomaly detection." *EPJ Nuclear Sciences & Technologies* (2019).

[5] A. Mylonakis, P. Vinai, and C. Demazière. "CORE SIM+: A flexible diffusion-based solver for neutron noise simulations." *Annals of Nuclear Energy*, **volume 155**, p. 108149 (2021). URL https://www.sciencedirect.com/science/article/pii/S0306454921000256.

[6] C. Demazière and A. Dokhane. "Description of scenarios for the simulated data." *Technical Report D3 1* (2019).

[7] P. Kaul, D. De Martini, M. Gadd, and P. Newman. "RSS-Net: Weakly-Supervised Multi-Class Semantic Segmentation with FMCW Radar." *arXiv preprint arXiv:200403451* (2020).

[8] B. Wang, Y. Lei, S. Tian, T. Wang, Y. Liu, P. Patel, A. B. Jani, H. Mao, W. J. Curran, T. Liu, et al. "Deeply supervised 3D fully convolutional networks with group dilated convolution for automatic MRI prostate segmentation." *Medical physics*, **volume 46**(4), pp. 1707–1718 (2019).

[9] R. Liu, J. Lehman, P. Molino, F. Petroski Such, E. Frank, A. Sergeev, and J. Yosinski. "An intriguing failing of convolutional neural networks and the coordconv solution." *Advances in neural information processing systems*, **volume 31**, pp. 9605–9616 (2018).

[10] T.-Y. Lin, P. Goyal, R. Girshick, K. He, and P. Dollár. "Focal loss for dense object detection." In *Proceedings of the IEEE international conference on computer vision*, pp. 2980–2988 (2017).

[11] Y. Sun, E. Tzeng, T. Darrell, and A. A. Efros. "Unsupervised domain adaptation through self-supervision." *arXiv preprint arXiv:190911825* (2019).

[12] G. Ioannou, T. Tasakos, A. Mylonakis, G. Alexandridis, C. Demazière, P. Vinai, and A. Stafylopatis. "Feature extraction and identification techniques for the alignment of perturbation simulations with power plant measurements." In *International Conference on Mathematics & Computational Methods Applied to Nuclear Science & Engineering (M&C 2021). pre-print* (2021).